Am J Physiol Cell Physiol 305: C377–C391, 2013.
First published June 12, 2013; doi:10.1152/ajpcell.00404.2012.

CALL FOR PAPERS | *Stem Cell Physiology and Pathophysiology*

Functional expression of smooth muscle-specific ion channels in TGF-β_1-treated human adipose-derived mesenchymal stem cells

Won Sun Park,[1]* Soon Chul Heo,[2]* Eun Su Jeon,[2] Da Hye Hong,[1] Youn Kyoung Son,[1] Jae-Hong Ko,[3] Hyoung Kyu Kim,[4] Sun Young Lee,[4] Jae Ho Kim,[2]* and Jin Han[4]*

[1]*Department of Physiology, Kangwon National University School of Medicine, Chuncheon, Korea;* [2]*Medical Research Center for Ischemic Tissue Regeneration, Medical Research Institute, Department of Physiology, School of Medicine, Pusan National University, Yangsan, Korea;* [3]*Department of Physiology, Chung-Ang University, Seoul, Korea; and* [4]*National Research Laboratory for Mitochondrial Signaling, Department of Physiology, College of Medicine, Cardiovascular and Metabolic Disease Center, Inje University, Busan, Korea*

Submitted 17 December 2012; accepted in final form 7 June 2013

Park WS, Heo SC, Jeon ES, Hong DH, Son YK, Ko JH, Kim HK, Lee SY, Kim JH, Han J. Functional expression of smooth muscle-specific ion channels in TGF-β_1-treated human adipose-derived mesenchymal stem cells. *Am J Physiol Cell Physiol* 305: C377–C391, 2013. First published June 12, 2013; doi:10.1152/ajpcell.00404.2012.—Human adipose tissue-derived mesenchymal stem cells (hASCs) have the power to differentiate into various cell types including chondrocytes, osteocytes, adipocytes, neurons, cardiomyocytes, and smooth muscle cells. We characterized the functional expression of ion channels after transforming growth factor-β_1 (TGF-β_1)-induced differentiation of hASCs, providing insights into the differentiation of vascular smooth muscle cells. The treatment of hASCs with TGF-β_1 dramatically increased the contraction of a collagen-gel lattice and the expression levels of specific genes for smooth muscle including α-smooth muscle actin, calponin, smooth mucle-myosin heavy chain, smoothelin-B, myocardin, and *h*-caldesmon. We observed Ca^{2+}, big-conductance Ca^{2+}-activated K^+ (BK_{Ca}), and voltage-dependent K^+ (K_v) currents in TGF-β_1-induced, differentiated hASCs and not in undifferentiated hASCs. The currents share the characteristics of vascular smooth muscle cells (SMCs). RT-PCR and Western blotting revealed that the L-type ($Ca_v1.2$) and T-type ($Ca_v3.1$, 3.2, and 3.3), known to be expressed in vascular SMCs, dramatically increased along with the $Ca_v\beta_1$ and $Ca_v\beta_3$ subtypes in TGF-β_1-induced, differentiated hASCs. Although the expression-level changes of the β-subtype BK_{Ca} channels varied, the major α-subtype BK_{Ca} channel ($K_{Ca}1.1$) clearly increased in the TGF-β_1-induced, differentiated hASCs. Most of the K_v subtypes, also known to be expressed in vascular SMCs, dramatically increased in the TGF-β_1-induced, differentiated hASCs. Our results suggest that TGF-β_1 induces the increased expression of vascular SMC-like ion channels and the differentiation of hASCs into contractile vascular SMCs.

human adipose tissue-derived mesenchymal stem cells; TGF-β_1; ion channel; vascular smooth muscle

TISSUE ENGINEERS HIGHLIGHT mesenchymal stem cells (MSCs) because of their long-term viability, ability to renew, and potential to differentiate into diverse cell types. MSCs come from blood and various tissues, including bone marrow, umbilical cord blood, periosteum, amniotic fluid, skeletal muscle, synovium, and adipose tissues (5, 6, 20, 27a, 50, 53, 54, 57). MSCs can differentiate into several types of cells including chondrocytes, osteocytes, adipocytes, neuron, cardiomyocytes, and smooth muscle cells (SMCs; Refs. 11, 16, 23, 26, 47, 53, 55). Transforming growth factor-β (TGF-β; Refs. 28, 64), sphingosylphosphotylcholine (SPC; Refs. 22, 23), thromboxane A_2 (26), mechanical stress (32), coculture with vascular endothelial cells (4), and $PGF_{2\alpha}$ (35) can cause MSCs to differentiate into SMCs.

The specific expression of contractile proteins; for example, calponin, α-smooth muscle actin (α-SMA), smooth muscle-myosin heavy chain (SM-MHC), smoothelin, and *h*-caldesmon (23, 49, 56) characterizes the phenotypes of SMCs. These proteins are closely related to vascular development and cardiovascular diseases including atherosclerosis and hypertension (37, 49).

The expression of ion channels that regulate the contractile response, such as L-type Ca^{2+} channels, big-conductance Ca^{2+}-activated K^+ (BK_{Ca}) channels, and voltage-dependent K^+ (K_v) channels, also discriminates vascular SMCs from other cells. L-type Ca^{2+} channels play a key role in vascular smooth muscle contraction by inducing the influx of extracellular Ca^{2+} (15, 17). The characteristics of vascular Ca^{2+} channels are relatively small amplitude and slow activation and inactivation processes compared with neurons and cardiac myocytes. In SMCs, particularly vascular SMCs, BK_{Ca} channels are more highly expressed than small-conductance Ca^{2+}-activated K^+ (SK_{Ca}) and intermediate-conductance Ca^{2+}-activated K^+ (IK_{Ca}) channels (48). The physiological role of BK_{Ca} channels in vascular SMCs maintains myogenic tone. Membrane depolarization and intracellular Ca^{2+} activate BK_{Ca} channels counteracting the membrane depolarization and constriction caused by vasoconstrictors and pressure (8, 30, 48). The slow inactivation of K_v channels is also a specific characteristic of vascular SMCs. In general, the vascular K_v channels slowly decay with a time constant of ~1 s at >40 mV due to their intrinsic inactivation (48, 52).

Although previous studies clearly revealed that TGF-β_1, SPC, and thromboxane A_2 induced the differentiation of human adipose tissue-derived MSCs (hASCs) into smooth mus-

* W. S. Park and S. C. Heo contributed equally to this work, and J. H. Kim and J. Han contributed equally to this work.

Address for reprint requests and other correspondence: J. Han, National Research Laboratory for Mitochondrial Signaling, Dept. of Physiology, College of Medicine, Cardiovascular and Metabolic Disease Center, Inje Univ., 633-165 Gaegeum-dong, Busanjin-gu, Busan 613-735, Korea (e-mail: phyhanj@inje.ac.kr).

cle-like cells (22, 23, 26), no studies addressed the functional expression of SMC-specific ion channels in these cells. Therefore, we characterized for the first time the functional expression of ion channels during the TGF-β_1-induced differentiation of hASCs into vascular SMCs and found that differentiated hASCs functionally expressed vascular L-type Ca^{2+} channels, BK_{Ca} channels, and K_v channels.

MATERIALS AND METHODS

Materials. Phosphate-buffered saline, trypsin, α-MEM, and fetal bovine serum were purchased from Invitrogen (Carlsbad, CA). Carbachol was purchased from BIOMOL (Plymouth Meeting, PA). Rat tail collagen (type I) was purchased from BD Biosciences (Bedford, MA). BayK 8644, nicardipine, and iberiotoxin were purchased from Tocris Bioscience (Ellisville, MO). Anti-α-SMA (A2547) and anti-calponin (C2687) antibodies were purchased from Sigma-Aldrich (St. Louis, MO). Antibodies against myocardin (ab22621), anti-smoothelin-B (ab8969), anti-*h*-caldesmon (ab50016), anti-SM-MHC (ab53219), and glyceraldehyde-3-phosphate dehydrogenase (GAPDH) were purchased from Abcam (Cambridge, MA). Peroxidase-labeled secondary antibodies were purchased from Amersham Biosciences.

Culture of hASCs. Adipose tissue was obtained from elective surgeries with patient's informed written consent as approved by the

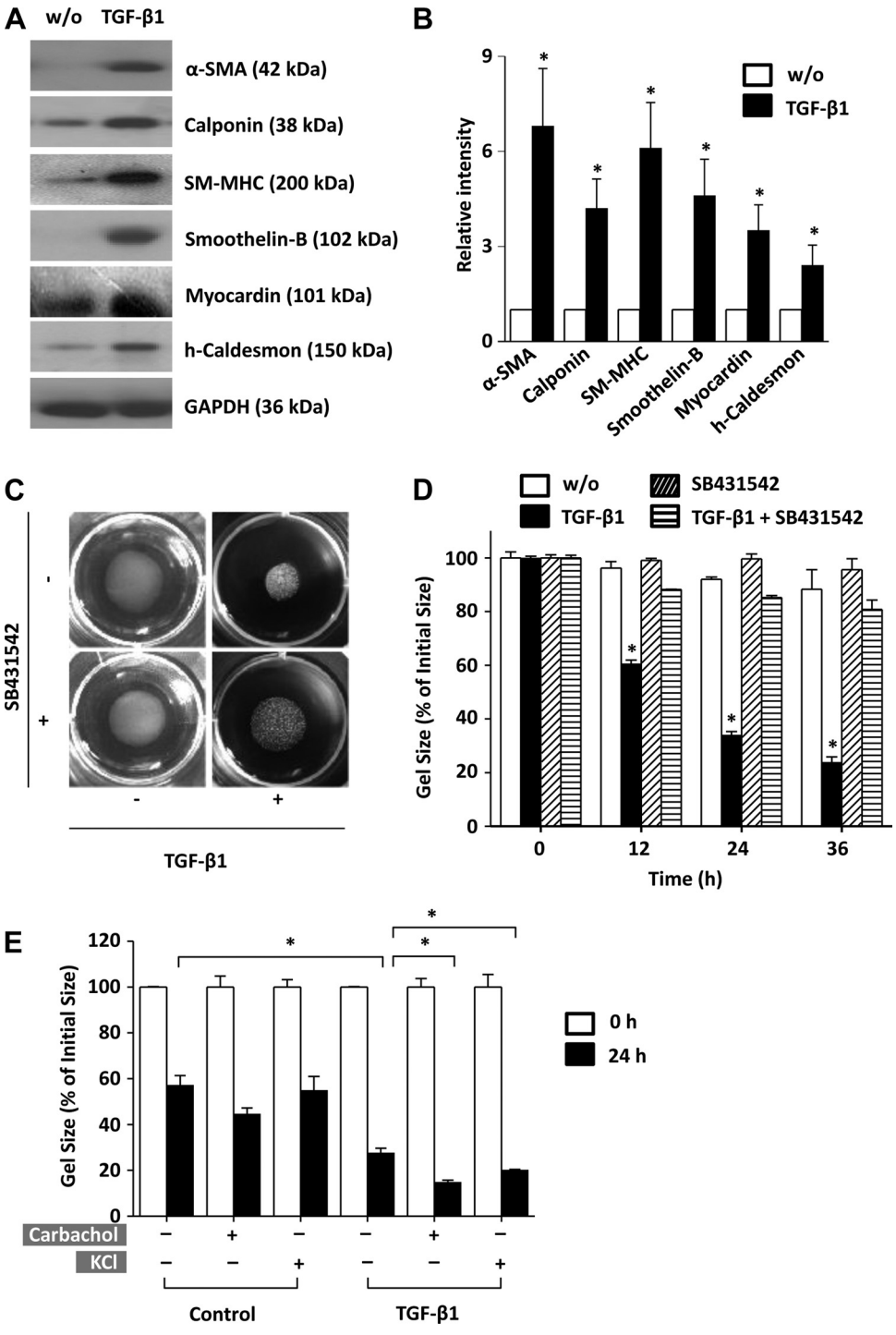

Fig. 1. Functional expression of smooth muscle cell (SMC) marker proteins and contractile-response of transforming growth factor-β_1-induced, differentiated human adipose tissue-derived mesenchymal stem cells (hASCs). *A*: expression of SMC-specific marker proteins in hASCs and transforming growth factor-β_1 (TGF-β_1)-induced, differentiated hASCs was determined by Western blotting. To ensure equal loading of each sample, the expression levels of GAPDH were determined. SM-MHC, smooth myosin heavy chain. *B*: statistical summary of *A*. $*P < 0.05$ vs. respective controls (w/o; $n = 4$). *C*: contractile response of hASCs and TGF-β_1-induced, differentiated hASCs. hASCs were treated with TGF-β_1 in the absence or presence of 10 μM SB432542 for 4 days and embedded into collagen gel lattices. Gel contraction was photographed at 24 h by using a digital camera. *D*: statistical summary of gel contraction, determined by Scion Image software ($n = 4$). The relative area of the gel lattices was obtained by dividing the area by the initial area of the lattice at each time point. $*P < 0.05$ vs. w/o (undifferentiated hASCs). *E*: undifferentiated hASCs (control) or TGF-β_1-induced, differentiated hASCs were embedded into collagen gel lattices. Collagen gels were exposed to 1 μM carbachol or 60 mM KCl for 24 h, and the area of gel lattices was determined at 0 and 24 h. The relative area of the gel lattices was obtained by dividing the area by the initial area of the lattice at 24 h ($n = 5$). $*P < 0.05$, by two-way ANOVA and Scheffé's post hoc test.

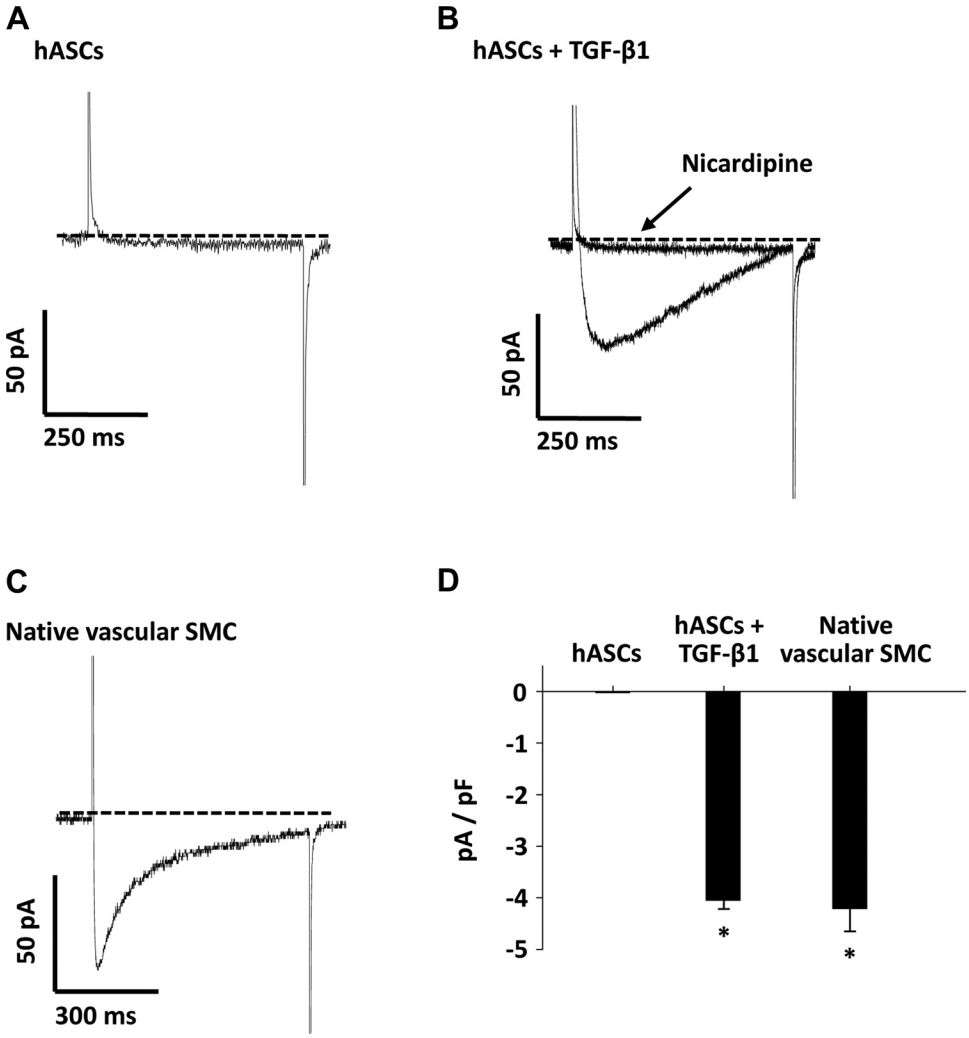

Fig. 2. Ba^{2+}-sensitive inward current in hASCs and TGF-β_1-induced, differentiated hASCs. The Ba^{2+}-sensitive L-type Ca^{2+} currents in the presence of the L-type Ca^{2+} channel agonist BayK 8644 (10 μM) were evoked by applying 500-ms depolarizing pulses from a holding potential of −40 to 0 mV. Ba^{2+}-sensitive L-type Ca^{2+} current traces were recorded in undifferentiated hASCs (*A*) and TGF-β_1-induced, differentiated hASCs (*B*). Application of nicardipine completely inhibited the Ba^{2+}-sensitive L-type Ca^{2+} current. *C*: L-type Ca^{2+} current recorded from rabbit coronary arterial SMCs. *D*: summary of current density in hASCs, TGF-β_1-induced, differentiated hASCs, and native vascular SMCs ($n = 5$). *$P < 0.05$ vs. hASCs.

Institution Review Board of Pusan National University Hospital. Culture of hASCs was performed in the same way as described previously (42). Briefly, we washed liposuction tissues more than three times with phosphate-buffered saline and mixed them with an equal volume of collagenase (type I) suspension (1 g/l buffered saline solution buffer with 1% bovine serum albumin) for 60 min at 37°C with shaking. Floating adipocytes were separated from the stromal-vascular fraction by centrifugation (300 *g* for 5 min). The cellular pellet was resuspended in MEM supplemented with 100 U/ml penicillin, 10% fetal bovine serum, and 100 μg/ml streptomycin, and cells were plated in dishes for tissue culture at 3,500 cells/cm^2. The primary hASCs were cultured for 4 or 5 days until they reached confluence, defined as passage "0". hASCs ware used between passages 3 and 10 in our experiments. The hASCs were positive for CD29, CD44, CD73, CD90, and CD105 and negative for CD31, CD34, and CD45. For TGF-β_1-induced differentiation of hASCs into SMCs,

Table 1. *List of Ca^{2+} channel primers for RT-PCR*

Subtype	Accession No.	Sense Primer (5′ to 3′)	Antisense Primer (5′ to 3′)
$Ca_v1.1$	NM_000069	AACGCCAAGAGGAGTATTATG	ATGGCTGTTGCTATGGTTGC
$Ca_v1.2$	NM_000719	CTGCAGGTGATGATGAGGTC	GCGGTGTTGTTGGCGTTGTT
$Ca_v1.3$	NM_000720	GCATTGGGAACCTCGAGCATGTGTCTG	GCGAGCTGTCATCCTCGTAGC
$Ca_v1.4$	NM_005183	GTGTCTCTGCCTGTCGG	TGCGCAGTGGGCCACTG
$Ca_v2.1$	NM_000068	CGATGCCTCAGGGAACACTTGG	CCATGTACCCATTGAGCTCACG
$Ca_v2.2$	NM_000718	GGAACCTGGTGGTGTCCCTGC	GGTTGTCCACAGCGATGG
$Ca_v2.3$	NM_000721	GGCATCCTGGCCACTGCAGG	CATCATTGGTATTGTACAGC
$Ca_v3.1$	NM_018896	GAAGTGCTACAGGGTGGAGGC	CCAGGTCTGCTGGGTCAGAGG
$Ca_v3.2$	NM_021098	GGAGAGCAACAAGGAGGCACG	AGTGCACAGAGGCAACGGAG
$Ca_v3.3$	NM_021096	CAAGGGGATGTGGCCTTGCC	TAGTAACGGTTCCAGTTGAC
$Ca_v\beta_1$	NM_000723	GTGAAGGAGGGCTGTGAGGTTG	GGTGTCAGCATCCAGAGCGAC
$Ca_v\beta_2$	NM_000724	GTGCAAACAGTGTAACGTCACCC	GCGACTTGTCCCACTGCGATG
$Ca_v\beta_3$	NM_000725	GAGTGACATTGGCAACCGACGC	GCAGGAGGCTGTCAGTAGCTATC
$Ca_v\beta_4$	NM_000726	GCAACTGGTTGTTCTTGATGC	GAGTTCTCTGTGGAGTGGTTG

hASCs were seeded onto six-well culture plates at 70% confluence, and they were treated with serum-free α-MEM in the absence or presence of 2 ng/ml TGF-β_1 for 96 h. Differentiation of hASCs into SMCs was characterized by Western blotting and electrophysiological analysis. For RT-PCR analysis of TGF-β_1-induced expression of smooth muscle-specific genes, hASCs were treated with serum-free α-MEM in the absence or presence of 2 ng/ml TGF-β_1 for 24 or 96 h.

Electrophysiological recordings. Electrophysiological recording was performed in a whole cell configuration using an Axopatch 1C amplifier (Axon Instruments, Union, CA) and digital interface (NI-DAQ 7; National Instruments, Union, CA). All experimental parameters were controlled by Patchpro software, which were developed by our group. The patch pipettes (Clark Electromedical Instruments, Pangbourne, UK) were pulled with two-step vertical puller (PP-83, Narishige, Tokyo, Japan) and had tip resistances of 3–4 MΩ with the filling of the pipette solution. The recorded signals were sampled at a rate of 1~3 kHz and filtered at 0.5~1.0 kHz.

The extracellular normal Tyrode solution for recordings of BK_{Ca} and K_v channels contained the following (in mM): 140 NaCl, 5.4 KCl, 1.8 $CaCl_2$, 0.33 NaH_2PO_4, 0.5 $MgCl_2$, 5 HEPES, and 16.6 glucose, adjusted to pH 7.4 with NaOH. The pipette-filled solution for recordings of BK_{Ca} channels contained the following (in mM): 115 K-aspartate, 5 NaCl, 25 KCl, 2 $MgCl_2$, 3 Mg-ATP, and 10 HEPES,

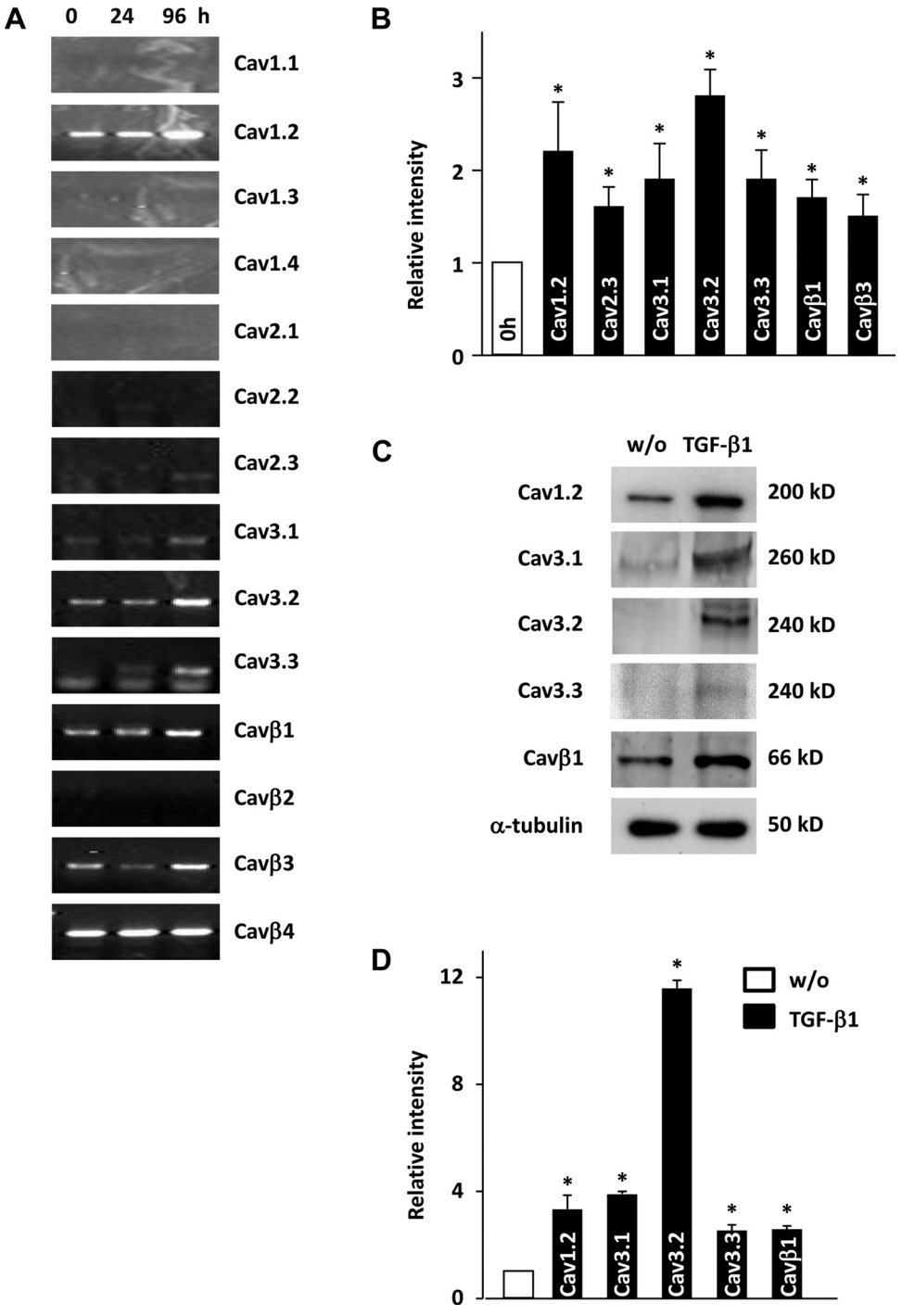

Fig. 3. Expression of Ca^{2+} channel subtypes in hASCs and TGF-β_1-induced, differentiated hASCs. *A*: mRNA expression of Ca^{2+} channel subtypes by RT-PCR. The expression levels of the $Ca_v1.2$, $Ca_v2.3$, $Ca_v3.1$, $Ca_v3.2$, $Ca_v3.3$, $Ca_v\beta_1$, and $Ca_v\beta_3$ subtypes were increased 96 h after TGF-β_1 treatment. *B*: summary of *A*. *$P < 0.05$ vs control (0 h; $n = 4$). *C*: Western blotting of the $Ca_v1.2$, $Ca_v3.1$, $Ca_v3.2$, $Ca_v3.3$, and $Ca_v\beta_1$ subtypes at 96 h after TGF-β_1 treatment. *D*: summary of *C*. All $n = 4$. *$P < 0.05$ vs. w/o (undifferentiated hASCs).

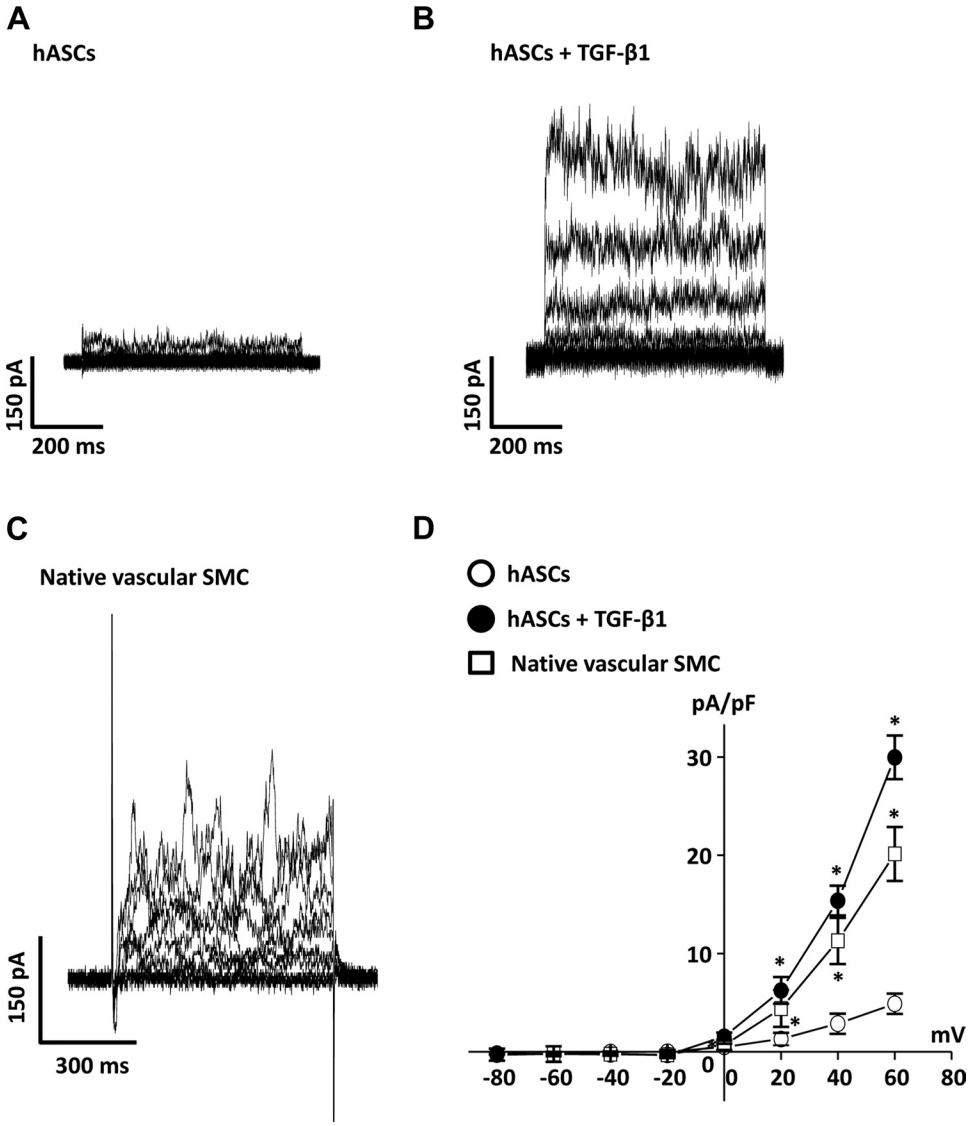

Fig. 4. Iberiotoxin-sensitive outward current in hASCs and TGF-β_1-induced, differentiated hASCs. The iberiotoxin-sensitive big-conductance Ca^{2+}-activated K^+ (BK_{Ca}) currents were obtained by applying step depolarizing pulses from −80 mV to +60 mV in step of 20 mV with a holding potential of −80 mV. Iberiotoxin-sensitive current was determined by subtracting the currents in the presence of iberiotoxin (100 nM) from those in the absence of iberiotoxin. *A*: iberiotoxin-sensitive current in undifferentiated hASCs. *B*: iberiotoxin-sensitive current in TGF-β_1-induced, differentiated hASCs. *C*: BK_{Ca} current recorded from rabbit coronary arterial SMCs. *D*: current-voltage (*I-V*) relationships of undifferentiated hASCs (○), TGF-β_1-induced, differentiated hASCs (●), and native vascular SMCs (□); $n = 4$. *$P < 0.05$ vs. hASCs.

adjusted to pH 7.25 with KOH. The pipette-filled solution for recordings of K_v channels contained the following (in mM): 105 K-aspartate, 5 NaCl, 25 KCl, 2 $MgCl_2$, 3 Mg-ATP, 10 BAPTA, and 10 HEPES, adjusted to pH 7.25 with KOH.

The Ba^{2+}-sensitive and voltage-dependent Ca^{2+} currents were recorded using nystatin-perforated patch clamp technique. For the perforated-patch recordings of Ca^{2+} currents, the cells bathed in a solution contained the following (in mM): 120 NaCl, 5 CsCl, 10

Table 2. *List of BK_{Ca} channel primers for RT-PCR*

Subtype	Accession No.	Sense Primer (5′ to 3′)	Antisense Primer (5′ to 3′)
$BK_{Ca}1.1$	NM_001014797	AGGAATGCATCTTGGCGTCACT	GCGGCAGCGGTCCCTATT
$BK_{Ca}2.1$	NM_002248	TGGAGGGGGCAGCTGAAGGAGAAC	CCGCCCCACGCTGCCATTGT
$BK_{Ca}2.2$	NM_170775	CCACCAATTCCGGACGCAGTA	GGGACCGCTCAGCATTGTAAGTG
$BK_{Ca}2.3$	NM_002249	AGCCACCGCATCCCCTGTCTCA	TGCCGGCATGCTGGTGGTTG
$BK_{Ca}3.1$	NM_002250	CACCCTAGCCCCTCCTTATTCTCA	CCGGGGTCTTGGGGCTCAG
$BK_{Ca}4.1$	NM_020822	AGACGCCAAGGCCTACGGGTTCAA	CTCGGCGCTCATGGTGCTCTCCTT
$BK_{Ca}\beta_1$	NM_004137	GGCGGCCCAGAAGTAGAGC	ATGCAGCCGGAAACAGGTATGAGT
$BK_{Ca}\beta_2$	NM_005832	CAAAGCGGCGAGTGGTGT	TCCCCGGAAGAAGTCAGGTTA
$BK_{Ca}\beta_{3a}$	NM_171828	CGAGGCGGAAACACAGG	GGCAAGGCGGAGCGGTCAGT
$BK_{Ca}\beta_{3b}$	NM_171829	CCCGAGGGCTGGTGGTGA	CCCGGCTCTCCTCCTGGTG
$BK_{Ca}\beta_{3c}$	NM_171830	CTGGGAGGCGGAGGAGGTT	TGGGGAAAGGGAGAAGGAGATACT
$BK_{Ca}\beta_e$	NM_001163677	TGATGAGCATAAACAGTAAGTG	TTTCTCTATATTTTGTCATTCAGT
$BK_{Ca}\beta_{3all}$	Homology	GCCGTGATGCTGGGGTTTG	TGGCAGTGCAGGTCGATTCTTCTC
$BK_{Ca}\beta_4$	NM_014505	CAGCGGGCGATGGAGACAGAGA	ACGACGCCGGAGATGATGAGAAAC

BK_{Ca}, big-conductance Ca^{2+}-activated K^+ current.

$BaCl_2$, 0.5 $MgCl_2$, 5 TEA-Cl, 10 HEPES, 10 glucose, and 0.01 BayK 8644, adjusted to pH 7.4 with NaOH. The pipette-filled solution contained the following (in mM): 130 CsCl, 10 EGTA, 10 HEPES, and 5 Mg-ATP, adjusted to pH 7.2 with CsOH. Nystatin (200 μg/ml) was added to the pipette solution every 2 h.

RT-PCR. Total cellular RNA was extracted using the mRNA isolation system (Novagen, Darmstadt, Germany), following the manufacturer's guideline. For the RT-PCR analysis, 2-μg RNA aliquots were subjected to cDNA synthesis with 200 U MMLV reverse transcriptase (Invitrogen) and 0.5 μg oligo (dT) 15 primer (Promega, Madison, WI). For the PCR reaction, 1 μl synthesized cDNA was used as a template. PCR primers were used to amplify human BK_{Ca}, Ca^{2+}, and K_v channels. The thermal cycle profile was as follows: 30-s denaturation at 95°C, 45-s annealing at 46–65°C, and extension for 45 s at 72°C with 0.5 U of GoTaq DNA polymerase (Promega, Madison, WI). This step was followed by extension step of 72°C for 10 min. For semiquantitative evaluation of expression levels, each PCR was performed for 30 cycles. PCR products were analyzed by 1.2% agarose gel electrophoresis and ethidium bromide staining.

Collagen lattice contraction model. Cell contractility was measured by trypsinized cells in monolayer cultures by treatment with trypsin-EDTA contained solution. Then, cells were counted and resuspended in α-MEM at a density of 1×10^6 cells/ml. After the cell suspension was mixed with collagen gel solution to make an experimental concentration of 3 mg collagen/ml and 4×10^5 cells/ml, we added the cell on the collagen mixture into 12-well culture plates (Nunc, Roskilde, Denmark). Under standard culture conditions, plates were incubated for 1 h to make collagen cell lattices and serum-free α-MEM was added into the plates. To initiate collagen gel contraction, lattices were added from the bottom of the culture dishes by

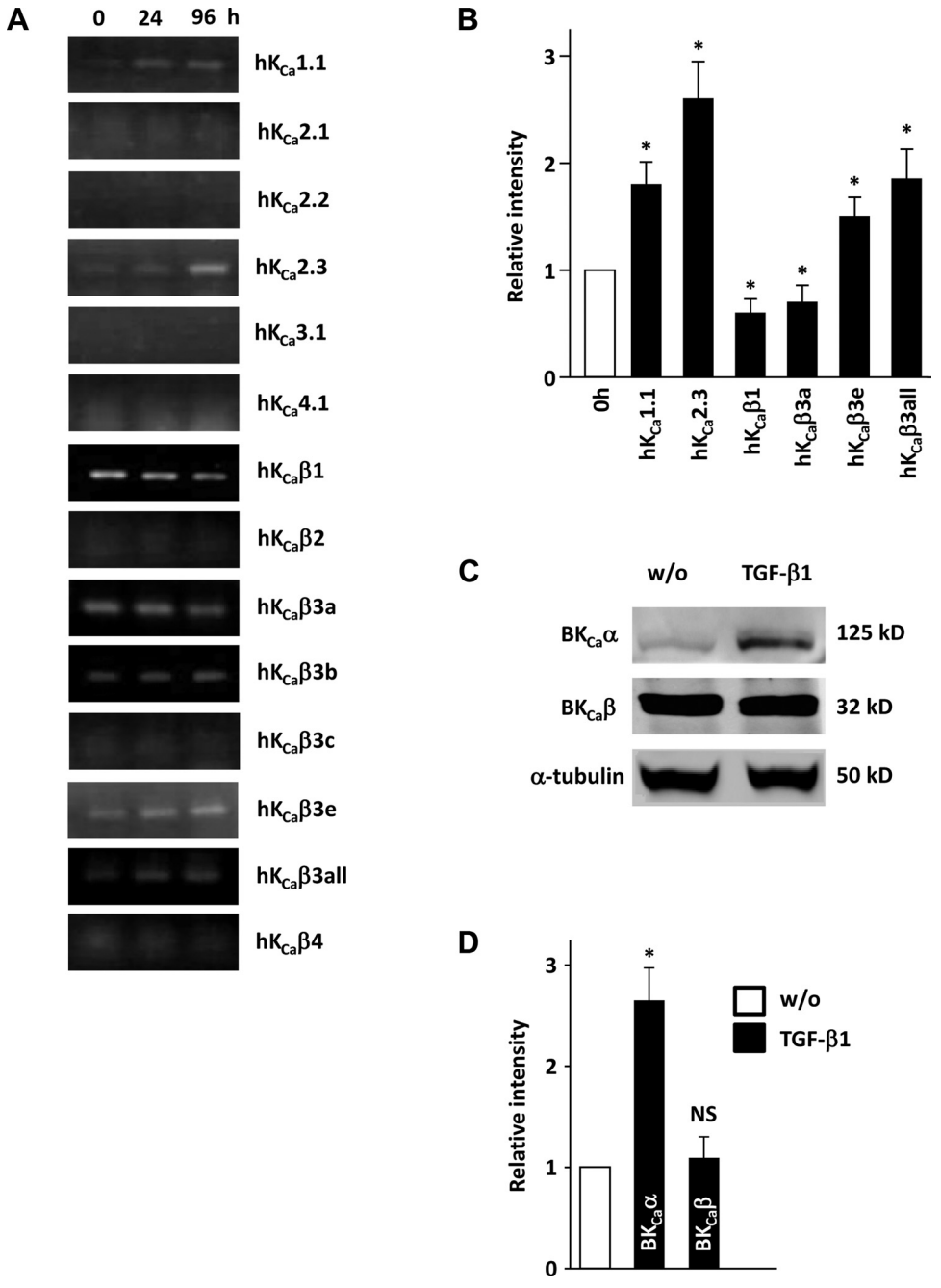

Fig. 5. Expression of BK_{Ca} channel subtypes in hASCs and TGF-β_1-induced, differentiated hASCs. *A*: comparison of mRNA expression levels for BK_{Ca} ($K_{Ca}1.1$), SKCa ($K_{Ca}2.X$), IKCa ($K_{Ca}3.1$) α-subunits, and β-subunits between hASCs and TGF-β_1-induced, differentiated hASCs. *B*: summary of *A*. $*P < 0.05$ vs control (0 h) ($n = 4$). *C*: Western blotting of $BK_{Ca}\alpha$ and $BK_{Ca}\beta$ subtypes at 96 h after TGF-β_1 treatment. *D*: summary of *C*. All $n = 4$. $*P < 0.05$ vs. w/o (undifferentiated hASCs).

gentle agitation at the lattice-dish interface after the addition of activators or inhibitors. The extent of gel contraction was analyzed by detecting the dimensions of the lattice using Scion Image software (compliments of Scion) (23).

Western blot. To prepare membrane fractions, cells were homogenized in lysis buffer containing the following (in mM): 150 NaCl, 20 Tris·HCl, 50 NaF, 10 EDTA, and 25 $NaVO_4$, and centrifuged at 12,000 rpm for 10 min. Extract was ultra-centrifuged again at 100,000 *g* for 1 h to separate the plasma membrane fraction. The pellet was homogenized in lysis buffer containing the following (in mM): 150 NaCl, 20 Tris·HCl, 50 NaF, 10 EDTA, 25 $NaVO_4$, and 1% Triton X-100. Equal amounts of membrane proteins (30 μg) were separated by 8% SDS-PAGE and were electrophoretically transferred to nitrocellulose membranes. The blocked membrane was incubated with antibodies to $Ca_v1.2$ (Sigma), $Ca_v3.1$ (Alomone Laboratories), $Ca_v3.2$ (Alomone Laboratories), $Ca_v3.3$ (Chemicon International), $Ca_v\beta_1$ (Santa Cruz Biotechnology, Santa Cruz, CA), $BK_{Ca}\alpha$ (BD Biosciences, San Diego, CA), $BK_{Ca}\beta$ (Abcam, Cambridge, MA), $K_v1.2$ (Abcam), $K_v1.5$ (Santa Cruz Biotechnology), $K_v3.2$ (Santa Cruz Biotechnology), and secondary antibodies, a goat anti-mouse IgG (Abcam) for $BK_{Ca}\alpha$ and rabbit anti-goat IgG (Abcam) for $Ca_v1.2$, $Ca_v3.1$, $Ca_v3.2$, $Ca_v3.3$, $Ca_v\beta_1$, $BK_{Ca}\beta$, $K_v1.2$, $K_v1.5$, and $K_v3.2$. Images were captured using a Fuji Imager LAS3000 at 75% of total resolution 10- to 60-s exposure and Multi-Gauge V2.3 system.

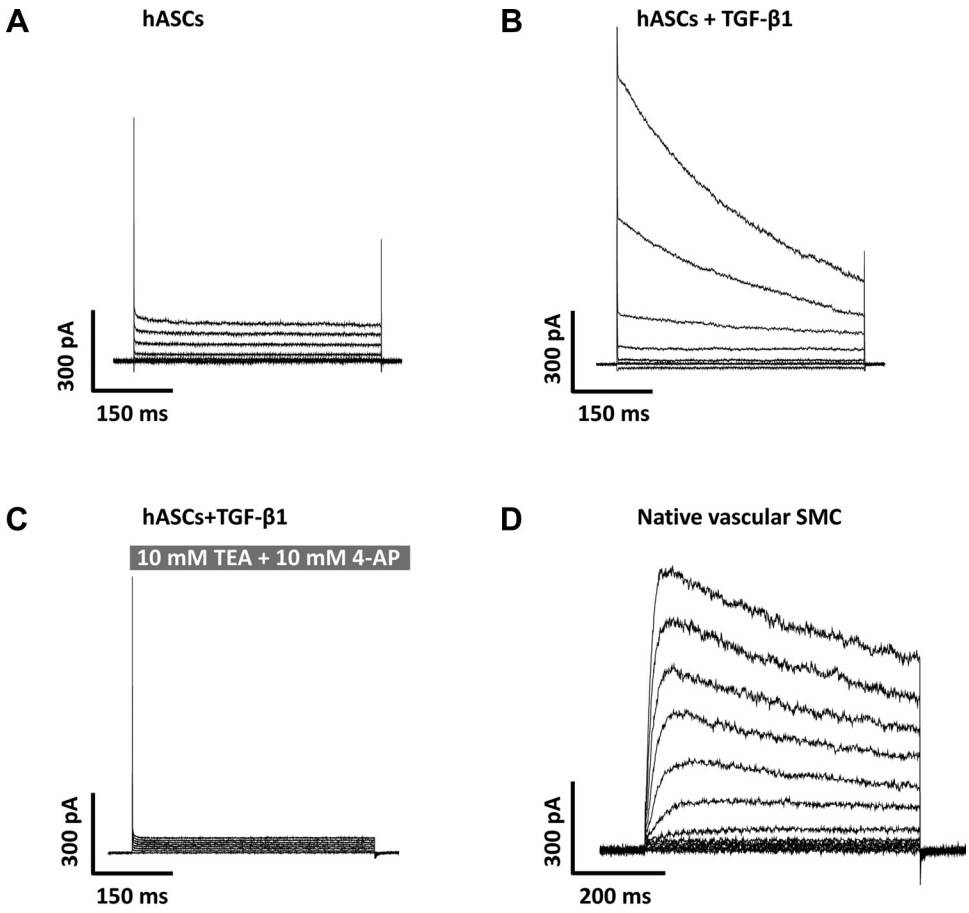

Fig. 6. Voltage-dependent K^+ current (K_v) in hASCs and TGF-β_1-induced, differentiated hASCs. Superimposed current traces were evoked by step depolarizing pulses between −80 mV and +60 mV in step of 20 mV from a holding potential of −80 mV. *A*: K_v current in undifferentiated hASCs. *B*: K_v current in TGF-β_1-induced, differentiated hASCs. *C*: K_v current in TGF-β_1-induced, differentiated hASCs with 10 mM TEA and 4-aminopyridine (4-AP). *D*: K_v current recorded from rabbit coronary arterial SMCs. *E*: *I-V* relationships of undifferentiated hASCs (○),TGF-β_1-induced, differentiated hASCs (●), and TGF-β_1-induced, differentiated hASCs with TEA and 4-AP (□); $n = 4$. $^*P < 0.05$.

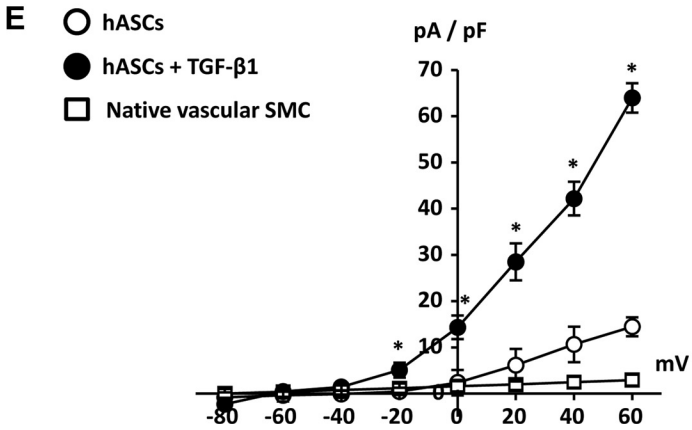

Hindlimb ischemia, cell transplantation, and blood flow measurement. Athymic nude mice (age 8–10 wk and weighing 17–22 g) were anesthetized with 160 mg/kg pentobarbital injection. The femoral artery was excised from its proximal origin. After arterial ligation, mice were divided by following experimental groups: the TGF-β_1-treated hASCs, the serum-starved hASCs, and the vehicle group (saline buffer; $n = 8$ per each group). In each animal, 3×10^6 cells (200 μl) or medium (DMEM) was injected intramuscularly into four points of the gracilis muscle located in the medial thigh. The extent of necrosis in ischemic hindlimb was recorded on *day 28* after surgery. The scores of necrosis were evaluated as follows: 0, limb salvage; 1, toes amputation; 2, foot amputation; and 3, limb amputation. Blood flow of the normal and ischemic limb was measured by laser Doppler perfusion imaging (LDPI) analyzer (Moor instruments, Devon, UK) on *days 0*, *7*, *14*, *21*, and *28* after hindlimb ischemia. The perfusion of the nonischemic and ischemic limb was presented as colored histogram pixels. Red and blue colors indicate high and low perfusion, respectively. Blood perfusion is expressed as the LDPI index representing the ratio of ischemic vs. nonischemic limb blood flow. A ratio of 1 before operation indicates equal blood perfusion of both legs.

Histological and immunofluorescence analyses. After blood flow measurement was completed over 28 days, hindlimb muscles were removed, formalin-fixed, and paraffin-embedded. Tissues were sliced into 5-μm sections, and endothelial cells and SMCs were identified by immunostaining with rat anti-CD31 (550274; BD Pharmingen) and rabbit anti-α-SMA (ab5694; Abcam) antibodies and then followed by incubation with Alexa 488 goat anti-rat and Alexa 488 goat anti-rabbit secondary antibodies, respectively. The specimens were washed and mounted in Vectashield medium (Vector Laboratories) with DAPI for visualization of nuclei. The stained sections were visualized by laser scanning confocal microscopy (Olympus FluoView FV1000). Capillary density was assessed by counting the number of CD31-positive features per high-power field (×400). Nine mice from each experimental group were analyzed. Twelve randomly selected microscopic fields from three serial sections in each block were examined for the existence of capillary endothelial cells.

Data analysis and statistics. Origin 6.0 software (Microcal Software, Northampton, MA) was used for data analysis. For statistical analysis of the data, Student's *t*-test, two-way ANOVA, and Scheffé's post hoc test were used to test for statistical significance. The results are expressed as means ± SE. We considered $P < 0.05$ to be statistically significant.

RESULTS

TGF-β_1-induced differentiation of hASCs to SMCs. To test whether hASCs could be differentiated into SMCs by TGF-β_1, we exposed hASCs to TGF-β_1 for 4 days. As shown in Fig. 1, *A* and *B*, the expression levels of SMC-specific contractile proteins (α-SMA, calponin, SM-MHC, smoothelin-B, myocardin, and *h*-caldesmon) and smooth muscle-specific transcription factor myocardin dramatically increased after treatment with TGF-β_1. Although we detected most of the proteins in various SMCs, including visceral and vascular SMCs, vascular SMCs predominantly expressed smoothelin-B (102 kDa); visceral SMCs express a different isoform: smoothelin-A (59 kDa) (23, 59). We detected only smoothelin-B after the TGF-β_1-induced differentiation of hASCs into SMCs, suggesting that the differentiated SMCs were vascular SMCs.

Collagen lattice contraction assay is useful for measuring the contractile force of cells (23). As shown in Fig. 1, *C* and *D*, treating the hASCs with TGF-β_1 to differentiate them into vascular SMCs reduced the size of the collagen lattices in a time-dependent manner. Undifferentiated hASCs and/or pretreated with the TGF-β antagonist SB431542 (10 μM) did not contract. We also evaluated the contractility of TGF-β_1-induced, differentiated hASCs after treatment with a contractile agonist (1 μM carbachol) and membrane depolarization (60 mM KCl). As shown in Fig. 1*E*, carbachol or high KCl strongly shrank the collagen lattices of the TGF-β_1-induced,

Table 3. *List of K_v channel primers for RT-PCR*

Subtype	Accession No.	Sense Primer (5′ to 3′)	Antisense Primer (5′ to 3′)
$K_v1.1$	L02750	CATCTGGTTCTCCTTCGAGC	GTTAGGGGAACTGACGTGGA
$K_v1.2$	L02752	TCCGGGATGAGAATGAAGAC	TTGGACAGCTTGTCACTTGC
$K_v1.3$	M55515	GTTCTCCTTCGAACTGCTGG	CTGAAGAGGAGAGGTGCTGG
$K_v1.4$	M55514	CCCCAGCTTTGATGCCATCTTG	TGAGGATGGCAAAGGACATGGC
$K_v1.5$	M55513	TGCGTCATCTGGTTCACCTTCG	TGTTCAGCAAGCCTCCCATTCC
$K_v1.6$	X17622	TCAACAGGATGGAAACCAGCCC	CTGCCATCTGCAACACGATTCC
$K_v1.7$	AJ310479	TGCCCTTCAATGACCCGTTCTTC	AAGACACGCACCAATCGGATGAC
$K_v2.1$	L02840	TACAGCCTCGACGACAACG	ACCACGCGGCGGACATTCTG
$K_v2.2$	U69962	AACGAACTGAGGCGAGAG	ACTCCGCCTAAGGGTGAAAC
$K_v3.1$	S56770	AACCCCATCGTGAACAAGACGG	TCATGGTGACCACGGCCCA
$K_v3.2$	AI363404	CTGCTGCTGGATGACCTACC	TGTGCCATTGATGACTGGTT
$K_v3.3$	AF055989	TTCTGCCTGGAAACCCATGAGG	TGTTGACAATGACGGGCACAGG
$K_v3.4$	M64676	TTCAAGCTCACACGCCACTTCG	TGCCAAATCCCAAGGTCTGAGG
$K_v4.1$	AJ005898	ATCTCGAGGAGATGAGGTTC	TTCTTTCGGTCCCGATAC
$K_v4.3$	AF048712	TGGCTTCTTCATCGCTGTCTCG	CCGAAGATCTTCCCTGCAATCG
$K_v4.4$	NM_012283	AGCCAAGAAGAACAAGCTG	AGGAAGTTTAGGACATGCC
$K_v5.1$	AF033382	TCCACATGAAGAAGGGCATCTGC	TCACGTAGAAGGGGAGGATG
$K_v6.1$	AF033383	TGCACCAACTTCGACGACATCC	GGAACTCCAGGGAGAACCAGCC
$K_v6.2$	AJ0111021	AAGCTCTTCGCCTGCGTGTC	CAGCAGCAGCGACACGTAGAAC
$K_v6.3$	NM_172347	ATGCCCATGCCTTCCAGAGA	AGAGCTGCACGATCTCCTCG
$K_v8.1$	AF167082	TTCCACAGCTGCCCGTATCTTTG	TTTTGCCTGTGGTGGTGTCTGG
$K_v9.1$	AF043473	TTTGAGGACTTGCTGAGCAGCG	TTGCTCCAGGCACACCAACAAG
$K_v9.2$	XM_043106	GTACTGGGGCATCAACGAGT	CCACGGAGAGGTAGAGCAAG
$K_v9.3$	AF043472	CTCTGTGGGCATTTCCATTT	AGAAACAGGCACAAACACCC
$K_v10.1$	AF348982	GCTTGCCCGTCACTTCATTGGTC	TTCTTCCAGGCACTGTGATAGGA
$K_v11.1$	AF348983	AGCCATGCTCAAACAGAGTG	CTCCTCGTAGTCGTCGCACA

K_v, voltage-dependent K^+ current.

differentiated hASCs compared with undifferentiated hASCs. These results show that TGF-β_1-induced, differentiated hASCs exhibited the characteristics of SMCs.

Expression of voltage-dependent Ca^{2+} channels on TGF-β_1-induced differentiation of hASCs. Increased Ca^{2+} influx through voltage-dependent Ca^{2+} channels plays a crucial role in the contractile response of SMCs (1). To test whether L-type Ca^{2+} channels were functionally expressed during the TGF-β_1-induced differentiation of hASCs, we applied the patch-clamp technique to record the L-type Ca^{2+} channels directly. Figure 2 shows the Ba^{2+}-sensitive inward current in the presence of the L-type Ca^{2+} channel agonist BayK 8644 (10 μM) recorded during the TGF-β_1-induced differentiation of hASCs (Fig. 2, *B* and *D*) compared with the lack of inward current in the undifferentiated hASCs (Fig. 2, *A* and *D*). The inward current was almost abolished by the application of the L-type Ca^{2+} channel inhibitor nicardipine (1 μM; Fig. 2*B*). These results strongly suggest that L-type Ca^{2+} currents are highly expressed during the TGF-β_1-induced differentiation of hASCs. Furthermore, the recorded L-type Ca^{2+} channel amplitude and density were very similar to those of native vascular SMCs (Fig. 2, *C* and *D*), demonstrating that the TGF-β_1-induced, differentiated hASCs shared the characteristics of vascular SMCs. To further evaluate the molecular identity of the observed functional Ca^{2+} currents, we investigated the expression patterns in undifferentiated hASCs and TGF-β_1-induced, differentiated hASCs with specific primers (Table 1). Vascular SMCs express the major L-type ($Ca_v1.X$, specifically $Ca_v1.2$) Ca^{2+} channels (43) and a small portion of the T-type ($Ca_v3.X$) Ca^{2+} channels. Consistent with these facts, as shown in Fig. 3, *A* and *B*, the $Ca_v1.2$ and all Ca_v3 subtypes dramatically increased along with the $Ca_v\beta_1$ and $Ca_v\beta_3$ subtypes in TGF-β_1-induced, differentiated hASCs. Western blotting confirmed the increased representative Cav1.2, $Ca_v3.1$, $Ca_v3.2$, $Ca_v3.3$, and

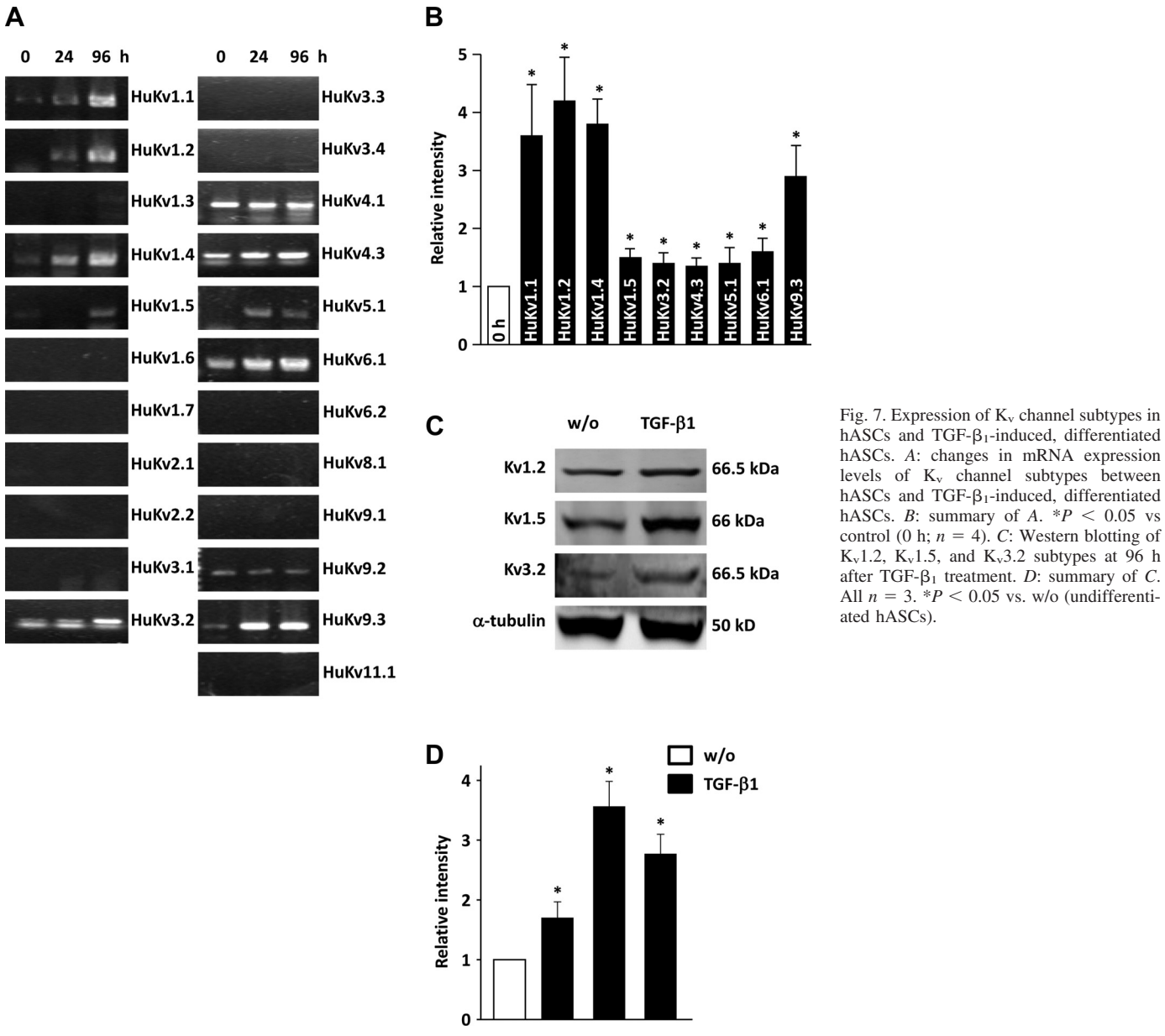

Fig. 7. Expression of K_v channel subtypes in hASCs and TGF-β_1-induced, differentiated hASCs. *A*: changes in mRNA expression levels of K_v channel subtypes between hASCs and TGF-β_1-induced, differentiated hASCs. *B*: summary of *A*. $*P < 0.05$ vs control (0 h; $n = 4$). *C*: Western blotting of $K_v1.2$, $K_v1.5$, and $K_v3.2$ subtypes at 96 h after TGF-β_1 treatment. *D*: summary of *C*. All $n = 3$. $*P < 0.05$ vs. w/o (undifferentiated hASCs).

$Ca_v\beta_1$ subtypes during the TGF-β_1-induced differentiation of hASCs (Fig. 3, *C* and *D*).

Expression of BK_{Ca} channels during TGF-β_1-induced differentiated hASCs. In vascular smooth muscle, the major outward currents activated at positive voltage are composed of BK_{Ca} and K_v channels (48). To identify the expression of BK_{Ca} channels, we applied iberiotoxin (100 nM), a specific BK_{Ca} channel inhibitor, on recorded outward current in hASCs and TGF-β_1-induced, differentiated hASCs. Figure 4 shows the lack of iberiotoxin-sensitive currents in hASCs (Fig. 4, *A* and *D*) and the abundance of noisy iberiotoxin-sensitive currents in TGF-β_1-induced, differentiated hASCs (Fig. 4, *B* and *D*). The current amplitude and electrophysiological characteristics were very similar to those of native vascular SMCs (Fig. 4, *C* and *D*), suggesting that TGF-β_1-induced hASCs differentiate into vascular SMCs. To further evaluate the molecular identity of the observed BK_{Ca} currents, we investigated the expression patterns of BK_{Ca} channels with specific BK_{Ca} channel primers (Table 2). As shown in Fig. 5, *A* and *B*, the TGF-β_1-induced differentiation of hASCs dramatically increased the expression levels of the major BK_{Ca} channel α-subtypes ($K_{Ca}1.1$) but not the SK_{Ca} channel α-subtypes ($K_{Ca}2.X$) and IK_{Ca} channel α-subtypes ($K_{Ca}3.1$). The expression levels of β-subtypes were relatively various. The expression of $BK_{Ca}\beta_1$, and $BK_{Ca}\beta_{3a}$ subtypes were slightly decreased in TGF-β_1-induced differentiation of hASCs. However, $BK_{Ca}\beta_{3e}$ and $BK_{Ca}\beta_3$ all subtypes were slightly increased. Consistent with the RT-PCR data, the Western blots also confirmed that the TGF-β_1-induced differentiation of hASCs increased the expression levels of the α-subtypes of BK_{Ca} but did not change the expression of the β-subtypes of BK_{Ca} (Fig. 5, *C* and *D*).

Expression of K_v channels during the TGF-β_1-induced differentiation of hASCs. K_v channels, which are activated by membrane depolarization and allow the efflux of K^+ to repolarize the membrane to the resting potential, are highly expressed in most vascular SMCs (31). To identify the expression of K_v channels, BK_{Ca} channels were inhibited by pretreatment of iberiotoxin (100 nM) in the extracellular solution and inclusion of BAPTA (10 mM), a Ca^{2+} chelator, in the pipette solution. As shown in Fig. 6, compared with the lack of K_v currents in hASCs (Fig. 6, *A* and *E*), the large K_v currents were recorded in TGF-β_1-induced, differentiated hASCs with intrinsic inactivation (Fig. 6, *B* and *E*), which is similar to native vascular SMCs (25, 48) (Fig. 6*D*). The general K_v channel inhibitors TEA (10 mM) and 4-aminopyridine (4-AP; 10 mM) nearly inhibited the large K_v currents recorded in the TGF-β_1-induced, differentiated hASCs (Fig. 6, *C* and *E*). These data also support that the TGF-β_1-induced, differentiated hASCs had the characteristics of vascular SMCs. Expression patterns of the K_v channel subtypes in TGF-β_1-induced, differentiated hASCs were investigated with specific primers (Table 3). As shown in Fig. 7, the TGF-β_1-induced differentiation of hASCs

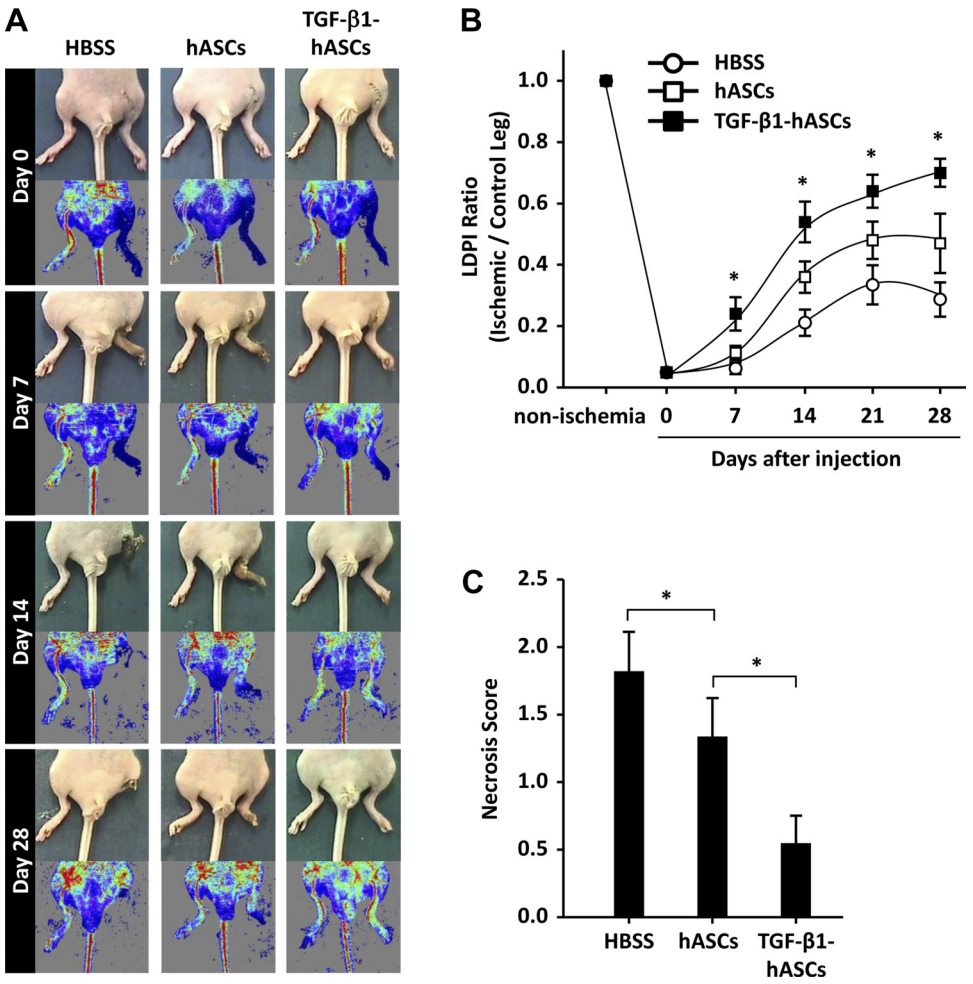

Fig. 8. Transplantation of TGF-β_1-treated hASCs promotes recovery from ischemia and reduces tissue necrosis in a hindlimb ischemia model. *A*: representative photographs and laser Doppler perfusion image (LDPI) blood perfusion images of mouse hindlimbs on *day 0*, *7*, *14*, and *28* after intramuscular injection of HBBS, serum-starved hASCs, or TGF-β_1-treated hASCs. *B*: quantitative analysis of the perfusion recovery was performed by LDPI. The LDPI index was evaluated as the ratio of ischemic to nonischemic hindlimb blood perfusion ($n = 8$ per group). $^*P < 0.05$ vs. serum-starved hASCs. *C*: statistical analysis of the necrosis score on *day 28* ($n = 8$ per group). $^*P < 0.05$.

dramatically increased the expression of the specific subtypes known to be expressed in vascular SMCs: $K_v1.1$, $K_v1.2$, $K_v1.4$, $K_v1.5$, and $K_v9.3$; the expression of the $K_v3.2$, $K_v4.3$, $K_v5.1$, and $K_v6.1$ subtypes also increased (Fig. 7, *A* and *B*). The representative Western blotting of the $K_v1.2$, $K_v1.5$, and $K_v3.2$ subtypes also showed increased expression levels in the TGF-β1-induced, differentiated hASCs (Fig. 7, *C* and *D*).

Transplantation of TGF-β1-treated hASCs stimulates blood perfusion of ischemic hindlimb through stimulating angiogenesis. To establish the therapeutic impact of TGF-β1-induced differentiation of hASCs into SMCs, TGF-β1-treated hASCs, serum-starved hASCs, or saline buffer were intramuscularly injected into the ischemic hindlimb, and blood flow was measured over a period of 4 wk using the LDPI analyzer. Intramuscular injection of TGF-β1-treated hASCs into the ischemic limb significantly improved blood perfusion, as judged by the LDPI. The LDPI ratio showed significant increase in mice transplanted with TGF-β1-treated hASCs, compared with the control groups in which serum-starved hASCs or saline buffer was injected (Fig. 8, *A* and *B*). Moreover, transplantation of TGF-β1-treated hASCs significantly inhibited tissue necrosis and amputation as shown by reduced necrosis score 4 wk after induction of ischemia and cell transplantation, compared with control groups (Fig. 8*C*).

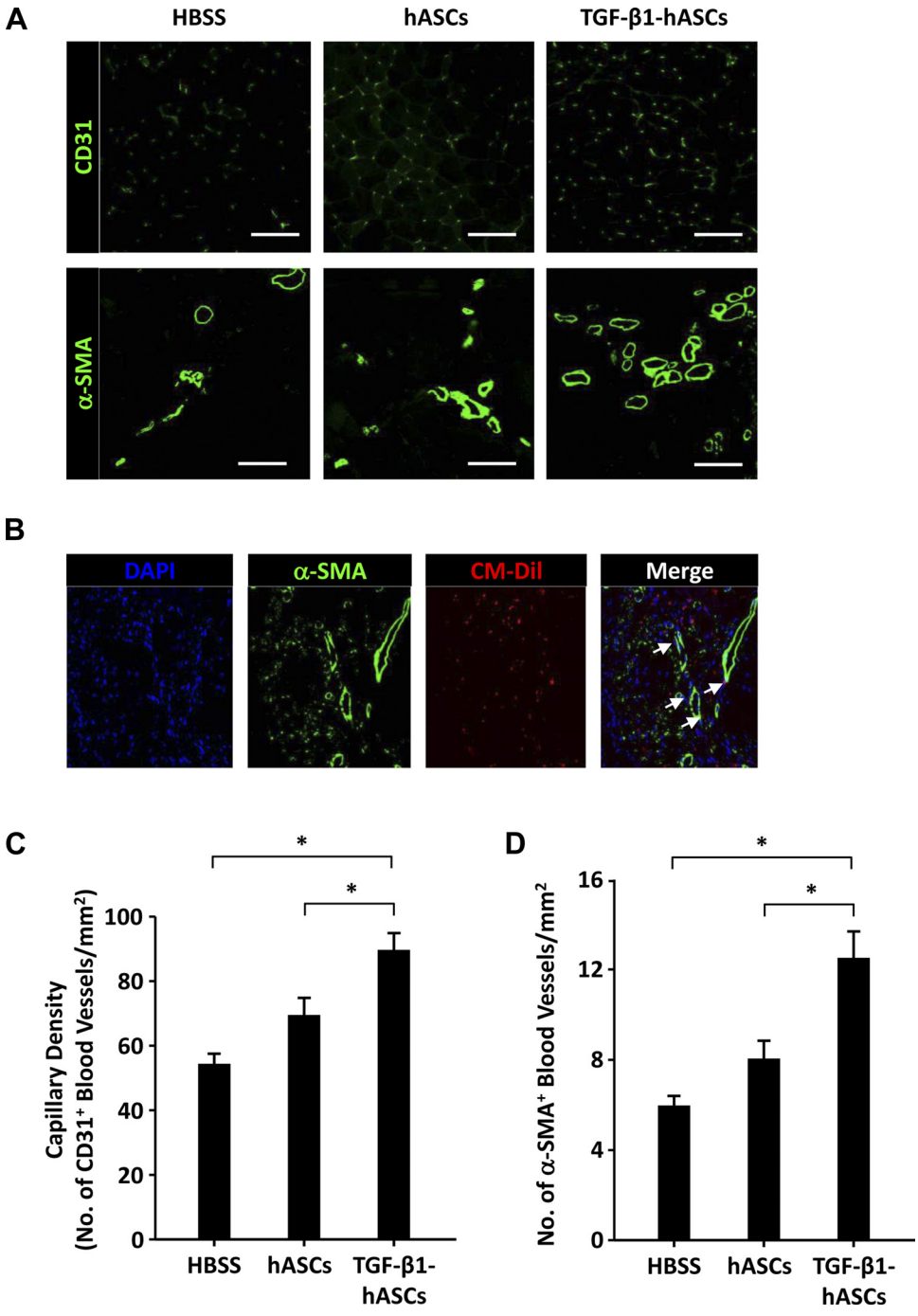

Fig. 9. Induction of neovascularization in vivo by the transplantation of TGF-β1-treated hASCs. *A*: immunofluorescence staining of ischemic hindlimb muscles with anti-CD31 and anti-α-SMA antibodies for staining of CD31-positive capillary blood vessels and α-SMA-positive arteries/arterioles. Bar = 50 μm. *B*: quantitative analysis of CD31-positive capillary density in ischemic hindlimb muscles. $^*P < 0.05$; $n = 40$. *C*: quantitative analysis of α-SMA-positive blood vessels in ischemic hindlimb muscles. $^*P < 0.05$; $n = 40$. *D*: α-SMA staining of ischemic hindlimb muscles on *day 28* after transplantation of TGF-β1-hASCs. Arrows indicate CM-DiI-positive staining in the α-SMA-positive blood vessels. Bar = 50 μm.

To assess whether transplantation of TGF-β_1-treated hASCs can stimulate angiogenesis in vivo, we determined densities of capillary and arterioles/arteries in ischemic muscle by immunostaining. CD31-positive capillary density was significantly higher in ischemic limb transplanted with TGF-β_1-treated hASCs than the control groups, which were injected with either serum-starved hASCs or saline buffer (Fig. 9, *A* and *B*). The densities of α-SMA-positive blood vessels were increased in ischemic limb injected with TGF-β_1-treated hASCs, compared with the control groups (Fig. 9, *A* and *C*). CD-DiI-labeled hASCs were detected in α-SMA-positive blood vessels (Fig. 9*D*). These findings of increased densities of CD31-positive capillary and α-SMA-positive arterioles/arteries after TGF-β_1-treated hASCs transplantation are consistent with the increased blood perfusion and reduced necrosis in the TGF-β_1-treated hASC-injected ischemic limb.

DISCUSSION

In this study, we directly compared the expression of Ca^{2+}, BK_{Ca}, and K_v channels at the mRNA, protein, and functional levels between undifferentiated hASCs and TGF-β_1-induced, differentiated hASCs. Our results show, based on changes in the expression levels of SMC-marker proteins and ion channels, that treating hASCs with TGF-β_1 induced them to differentiate into vascular SMCs.

The Ca^{2+} channels are classified into three families, Ca_v1 (L-types), Ca_v2 (P/Q, N, and R-types), and Ca_v3 (T-types) channels; L- and T-types Ca^{2+} channels are expressed in vascular smooth muscle (7, 18). Among the L-type Ca^{2+} channels, the $Ca_v1.2$ (*CACNA1C*) channel is the dominant isoform in vascular smooth muscle and therefore appears to play an important role in regulating vascular tone and arterial constriction (2, 45). Currently, the major targets of dihydropyridine Ca^{2+} channel blockers as antihypertensive drugs are the $Ca_v1.2$ channels expressed in vascular smooth muscle (43, 66). Therefore, the specific expression of $Ca_v1.2$ is an important characteristic of vascular smooth muscle. Our data clearly show, with support from the RT-PCR and Western blot results, that the expression level of the $Ca_v1.2$ subtype, and not other Ca_v1 subtypes, was dramatically increased in TGF-β_1-induced, differentiated hASCs (Fig. 3). Although low-voltage-activated T-type Ca^{2+} channels are typically expressed at low densities in vascular smooth muscle, the T-type Ca^{2+} channels play physiological roles in smooth muscle contraction, and therefore, modulating the T-type Ca^{2+} channels is one strategy to regulate hypertension and angina (13). For this reason, screening the T-type Ca^{2+} channel subtypes, the Ca_v3 families, is also essential method to verify the differentiation of vascular SMCs. Our data clearly show that the expression levels of all subtypes of the Ca_v3 family increased during the TGF-β_1-induced differentiation of hASCs. Although our study could not address the increase in the expression of the $Ca_v2.3$ (R-type, *CACNA1E*) channel in TGF-β_1-induced, differentiated hASCs, a previous study found $Ca_v2.3$ channels in the cerebral artery after subarachnoid hemorrhage, which contributed to enhanced cerebral-artery constriction and decreased cerebral blood flow (21).

Highly expressed BK_{Ca} channels in vascular SMCs regulate arteriolar tone under physiological conditions, and the alteration of BK_{Ca} channels is closely related to vascular diseases such as hypertension, hypertrophy, stroke, atherosclerosis, diabetes, and complications of cardiovascular surgery (14, 19, 27, 38, 39). The BK_{Ca} channel is composed of four pore-forming α-subunits ($K_{Ca}1.1$) and ancillary β-subunits at a 1:1 ratio (29, 58). A single gene, *KCNMA1* (or *slo1*), encodes the α-subunits that form the functional BK_{Ca} channel. A study of α-subunit-deleted ($Slo1^{-/-}$) mice revealed the absence of iberiotoxin-sensitive current in smooth muscle (41), suggesting that the increased expression levels and/or appearance of BK_{Ca}-channel α-subunits related directly to the increased BK_{Ca}-channel formation and occurrence of BK_{Ca} current. Our results clearly demonstrate an increase in BK_{Ca} channel α-subunit ($K_{Ca}1.1$) expression levels, with little expression of SK_{Ca} ($K_{Ca}2.X$) and IK_{Ca} ($K_{Ca}3.1$), and corresponding large iberiotoxin-sensitive outward currents in TGF-β_1-induced differentiated hASCs (Figs. 4 and 5). The Western blot data strongly support a dramatically increased expression level of the total α-subunit in the TGF-β_1-induced, differentiated hASCs. The β-subunits of the BK_{Ca} channel reportedly enhance the sensitivity of the channel to voltage and Ca^{2+} (40). Four isoforms (*KCNMB*1–4 or β_{1-4}) are identified as β-subunits in mammals. Among those, the β_1-subunit is highly expressed in smooth muscle including vascular SMCs (24, 38a). Our results suggest that the β_1-subunit is highly expressed in both undifferentiated hASCs and TGF-β_1-induced, differentiated hASCs, despite the fact that the expression level of the β_1-subunit slightly decreased during TGF-β_1-induced differentiation of the hASCs. The Western blot, however, revealed no difference in the total protein levels of the β-subunits between the undifferentiated hASCs and the TGF-β_1-induced, differentiated hASCs (Fig. 5). These results suggest that the β-subunits, but not the α-subunits, of the BK_{Ca} channel are affluent even in the undifferentiated state. After treatment of the hASCs with TGF-β_1 to differentiate them into vascular SMCs, the expression levels of the α-subunits dramatically increased, completing the BK_{Ca}-channel structure. Therefore, we observed the large BK_{Ca} current in the TGF-β_1-induced, differentiated hASCs (Fig. 4).

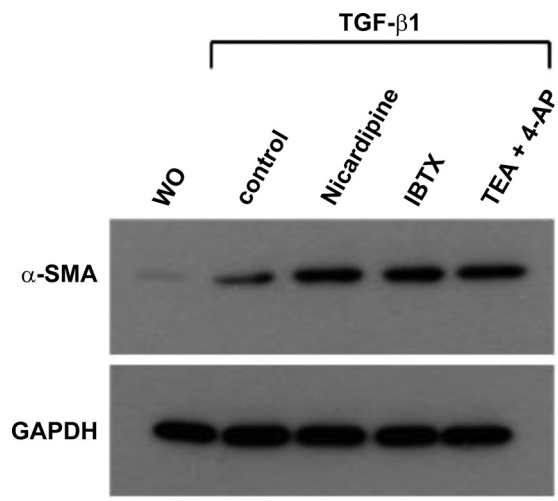

Fig. 10. Effects of Ca^{2+} and K^+ channel blockers on TGF-β_1-induced α-SMA expression. Serum-starved hASCs were treated with α-MEM in the absence (wo) or in the presence of 2 ng/ml TGF-β_1. During treatment with TGF-β_1, cells were treated with Nicardipine (1 μM), iberiotoxin (IBTX; 100 nM), TEA + 4-AP (each 10 mM), or vehicle (control) for 4 days.

The K_v channels consist of pore-forming α-subunits and ancillary β-subunits, similar to the BK_{Ca} channels (33). Although many studies addressed the physiological and pharmacological properties of vascular K_v channels, few examined the molecular subtypes of the K_v channels. Most studies of the molecular subtypes of K_v channels examined pulmonary arterial smooth muscle cells (PASMCs). In PASMCs, although other subtypes are controversial, several groups agree on the expression of the $K_v1.1$, $K_v1.2$, $K_v1.4$, $K_v1.5$, $K_v2.1$, and $K_v9.3$ subtypes (3, 9, 10, 51, 67). Our experiment clearly identified the expression of $K_v1.1$, $K_v1.2$, $K_v1.4$, $K_v1.5$, and $K_v9.3$, but not $K_v2.1$, in TGF-β_1-induced, differentiated hASCs. In general, K_v current in vascular SMCs slowly and partially decayed with a time constant of ~1 s at +40 mV, owing to intrinsic inactivation (48, 52). Concomitantly, the K_v current recorded in the TGF-β_1-induced, differentiated hASCs also showed a similar decay of current with a time constant of ~0.5 s at 40 mV. Taken together, the molecular subtypes and the intrinsic inactivation process of the K_v channels that we observed suggest that treating hASCs with TGF-β_1 causes them to differentiate into vascular SMCs.

TGF-β_1 has been reported to induce differentiation of mesenchymal stem cells into SMCs (34, 46, 63). The present study demonstrated that TGF-β_1 increased the expression of the SMC-specific transcription factor myocardin in hASCs. Myocardin plays an important role in the expression of SMC-specific genes by acting as a cofactor for serum-response factor (8a, 12, 65). It has been reported that mouse embryos lacking myocardin are difficult to survive during the early stage of smooth muscle development and fail to express genes for smooth muscle marker in embryonic dorsal aorta and other vascular structures (36). Forced expression of myocardin stimulated the expression of SMC markers in human mesenchymal stem cells (60, 61), whereas dominant negative myocardin mutants and myocardin-specific small interfering RNAs inhibited expression of SMC makers in SMCs (12, 65). Consistently, we have reported that TGF-β_3-induced expression of α-SMA in hASCs was abrogated by small interfering RNA-mediated silencing of myocardin and serum-response factor (22). Therefore, these results suggest that myocardin/serum-response factor-dependent mechanism plays a key role in TGF-β_1-induced differentiation of hASCs into SMCs.

Ca^{2+} and K^+ channels play a key role in not only regulation of smooth muscle contractility by eliciting an action potential but also expression of SMC-specific genes (62). We found that treatment of hASCs with the L-type Ca^{2+} channel blocker nicardipine, the BK_{Ca} channel blocker iberiotoxin, or the K_v channel blockers (4-AP + TEA) during incubation of the cells with TGF-β_1 had no significant impact on the differentiation of hASCs into SMCs (Fig. 10). These results suggest that these ion channels are not implicated in TGF-β_1-induced differentiation of hASCs into SMCs.

In the present study, we demonstrated for the first time that intramuscular injection of TGF-β_1-induced, differentiated hASCs significantly improved blood perfusion and neovascularization in the ischemic limb. Injection of TGF-β_1-treated hASCs increased formation of capillary and arterioles/arteries in ischemic limbs, and they incorporated into α-SMA-positive blood vessels. These results, together with the functional expression of ion channels, strongly suggest that TGF-β_1 treatment induces differentiation of hASCs into vascular SMCs. Although further studies of the physiological roles of ion channels in the differentiation of hASCs remain, our study will help to improve stem-cell research and stem-cell therapy in the near future.

GRANTS

This research was supported by the National Research Foundation of Korea (NRF) funded by the Ministry of Education, Science and Technology (2011-0019422, 2010-0021126, 2010-0020224, and 2012R1A2A1A03007595).

DISCLOSURES

No conflicts of interest, financial or otherwise, are declared by the author(s).

AUTHOR CONTRIBUTIONS

Author contributions: W.S.P., J.H.K., and J.H. conception and design of research; W.S.P., S.C.H., E.S.J., D.H.H., Y.K.S., J.-H.K., and S.Y.L. performed experiments; W.S.P., S.C.H., E.S.J., D.H.H., Y.K.S., J.-H.K., H.K.K., S.Y.L., J.H.K., and J.H. analyzed data; W.S.P., S.C.H., E.S.J., D.H.H., Y.K.S., J.-H.K., H.K.K., J.H.K., and J.H. interpreted results of experiments; W.S.P., S.C.H., E.S.J., Y.K.S., and J.H.K. prepared figures; W.S.P., Y.K.S., J.H.K., and J.H. drafted manuscript; W.S.P., H.K.K., J.H.K., and J.H. edited and revised manuscript; J.H.K. and J.H. approved final version of manuscript.

REFERENCES

1. **Abernethy DR, Soldatov NM.** Structure-functional diversity of human L-type Ca^{2+} channel: perspectives for new pharmacological targets. *J Pharmacol Exp Ther* 300: 724–728, 2002.
2. **Andreasen D, Friis UG, Uhrenholt TR, Jensen BL, Skott O, Hansen PB.** Coexpression of voltage-dependent calcium channels Cav1.2, 21a, and 21b in vascular myocytes. *Hypertension* 47: 735–741, 2006.
3. **Archer SL, Souil E, Dinh-Xuan AT, Schremmer B, Mercier JC, El Yaagoubi A, Nguyen-Huu L, Reeve HL, Hampl V.** Molecular identification of the role of voltage-gated K^+ channels, Kv1.5 and Kv21, in hypoxic pulmonary vasoconstriction and control of resting membrane potential in rat pulmonary artery myocytes. *J Clin Invest* 101: 2319–2330, 1998.
4. **Ball SG, Shuttleworth AC, Kielty CM.** Direct cell contact influences bone marrow mesenchymal stem cell fate. *Int J Biochem Cell Biol* 36: 714–727, 2004.
5. **Barry FP, Murphy JM.** Mesenchymal stem cells: clinical applications and biological characterization. *Int J Biochem Cell Biol* 36: 568–584, 2004.
6. **Bieback K, Kern S, Kluter H, Eichler H.** Critical parameters for the isolation of mesenchymal stem cells from umbilical cord blood. *Stem Cells* 22: 625–634, 2004.
7. **Braunstein TH, Inoue R, Cribbs L, Oike M, Ito Y, Holstein-Rathlou NH, Jensen LJ.** The role of L- and T-type calcium channels in local and remote calcium responses in rat mesenteric terminal arterioles. *J Vasc Res* 46: 138–151, 2009.
8. **Brayden JE, Nelson MT.** Regulation of arterial tone by activation of calcium-dependent potassium channels. *Science* 256: 532–535, 1992.
8a. **Chen J, Kitchen CM, Streb JW, Miano JM.** Myocardin: a component of a molecular switch for smooth muscle differentiation. *J Mol Cell Cardiol* 34: 1345–1356, 2002.
9. **Coppock EA, Martens JR, Tamkun MM.** Molecular basis of hypoxia-induced pulmonary vasoconstriction: role of voltage-gated K^+ channels. *Am J Physiol Lung Cell Mol Physiol* 281: L1–L12, 2001.
10. **Davies AR, Kozlowski RZ.** Kv channel subunit expression in rat pulmonary arteries. *Lung* 179: 147–161, 2001.
11. **Deans RJ, Moseley AB.** Mesenchymal stem cells: biology and potential clinical uses. *Exp Hematol* 28: 875–884, 2000.
12. **Du KL, Ip HS, Li J, Chen M, Dandre F, Yu W, Lu MM, Owens GK, Pamacek MS.** Myocardin is a critical serum response factor cofactor in the transcriptional program regulating smooth muscle cell differentiation. *Mol Cell Biol* 23: 2425–37, 2003.
13. **Ertel SI, Ertel EA, Clozel JP.** T-type Ca^{2+} channels and pharmacological blockade: potential pathophysiological relevance. *Cardiovasc Drugs Ther* 11: 723–739, 1997.
14. **Feng J, Liu Y, Khabbaz KR, Sodha NR, Osipov RM, Hagberg R, Alper SL, Sellke FW.** Large conductance calcium-activated potassium

channels contribute to the reduced myogenic tone of peripheral microvasculature after cardiopulmonary bypass. *J Surg Res* 157: 123–128, 2009.
15. **Fernandez-Tenorio M, Gonzalez-Rodriguez P, Porras C, Castellano A, Moosmang S, Hofmann F, Urena J, Lopez-Barneo J.** Short communication: genetic ablation of L-type Ca^{2+} channels abolishes depolarization-induced Ca^{2+} release in arterial smooth muscle. *Circ Res* 106: 1285–1289, 2010.
16. **Forbes SJ, Vig P, Poulsom R, Wright NA, Alison MR.** Adult stem cell plasticity: new pathways of tissue regeneration become visible. *Clin Sci (Lond)* 103: 355–369, 2002.
17. **Goto K, Kasuya Y, Matsuki N, Takuwa Y, Kurihara H, Ishikawa T, Kimura S, Yanagisawa M, Masaki T.** Endothelin activates the dihydropyridine-sensitive, voltage-dependent Ca^{2+} channel in vascular smooth muscle. *Proc Natl Acad Sci USA* 86: 3915–3918, 1989.
18. **Hansen PB, Jensen BL, Andreasen D, Skott O.** Differential expression of T- and L-type voltage-dependent calcium channels in renal resistance vessels. *Circ Res* 89: 630–638, 2001.
19. **Hill MA, Yang Y, Ella SR, Davis MJ, Braun AP.** Large conductance, Ca^{2+}-activated K^+ channels (BK_{Ca}) and arteriolar myogenic signaling. *FEBS Lett* 584: 2033–2042, 2010.
20. **In't Anker PS, Scherjon SA, Kleijburg-van der Keur C, Noort WA, Claas FH, Willemze R, Fibbe WE, Kanhai HH.** Amniotic fluid as a novel source of mesenchymal stem cells for therapeutic transplantation. *Blood* 102: 1548–1549, 2003.
21. **Ishiguro M, Wellman TL, Honda A, Russell SR, Tranmer BI, Wellman GC.** Emergence of a R-type Ca^{2+} channel (CaV 2.3) contributes to cerebral artery constriction after subarachnoid hemorrhage. *Circ Res* 96: 419–426, 2005.
22. **Jeon ES, Moon HJ, Lee MJ, Song HY, Kim YM, Bae YC, Jung JS, Kim JH.** Sphingosylphosphorylcholine induces differentiation of human mesenchymal stem cells into smooth-muscle-like cells through a TGF-beta-dependent mechanism. *J Cell Sci* 119: 4994–5005, 2006.
23. **Jeon ES, Park WS, Lee MJ, Kim YM, Han J, Kim JH.** A Rho kinase/myocardin-related transcription factor-A-dependent mechanism underlies the sphingosylphosphorylcholine-induced differentiation of mesenchymal stem cells into contractile smooth muscle cells. *Circ Res* 103: 635–642, 2008.
24. **Jiang Z, Wallner M, Meera P, Toro L.** Human and rodent MaxiK channel beta-subunit genes: cloning and characterization. *Genomics* 55: 57–67, 1999.
25. **Kim A, Bae YM, Kim J, Kim B, Ho WK, Earm YE, Cho SI.** Direct block by bisindolylmaleimide of the voltage-dependent K^+ currents of rat mesenteric arterial smooth muscle. *Eur J Pharmacol* 483: 117–126, 2004.
26. **Kim MR, Jeon ES, Kim YM, Lee JS, Kim JH.** Thromboxane A_2 induces differentiation of human mesenchymal stem cells to smooth muscle-like cells. *Stem Cells* 27: 191–199, 2009.
27. **Kim N, Chung J, Kim E, Han J.** Changes in the Ca^{2+}-activated K^+ channels of the coronary artery during left ventricular hypertrophy. *Circ Res* 93: 541–547, 2003.
27a. **Kim YS, Ahn Y.** A long road for stem cells to cure sick hearts: update on recent clinical trials. *Korean Circ J* 42: 71–79, 2012.
28. **Kinner B, Zaleskas JM, Spector M.** Regulation of smooth muscle actin expression and contraction in adult human mesenchymal stem cells. *Exp Cell Res* 278: 72–83, 2002.
29. **Knaus HG, Eberhart A, Glossmann H, Munujos P, Kaczorowski GJ, Garcia ML.** Pharmacology and structure of high conductance calcium-activated potassium channels. *Cell Signal* 6: 861–870, 1994.
30. **Ko EA, Han J, Jung ID, Park WS.** Physiological roles of K^+ channels in vascular smooth muscle cells. *J Smooth Muscle Res* 44: 65–81, 2008.
31. **Ko EA, Park WS, Firth AL, Kim N, Yuan JX, Han J.** Pathophysiology of voltage-gated K^+ channels in vascular smooth muscle cells: modulation by protein kinases. *Prog Biophys Mol Biol* 103: 95–101, 2010.
32. **Kobayashi N, Yasu T, Ueba H, Sata M, Hashimoto S, Kuroki M, Saito M, Kawakami M.** Mechanical stress promotes the expression of smooth muscle-like properties in marrow stromal cells. *Exp Hematol* 32: 1238–1245, 2004.
33. **Korovkina VP, England SK.** Molecular diversity of vascular potassium channel isoforms. *Clin Exp Pharmacol Physiol* 29: 317–323, 2002.
34. **Kurpinski K, Lam H, Chu J, Wang A, Kim A, Tsay E, Agrawal S, Schaffer DV, Li S.** Transforming growth factor-beta and notch signaling mediate stem cell differentiation into smooth muscle cells. *Stem Cells* 28: 734–42, 2010.
35. **Lee MJ, Kim MY, Heo SC, Kwon YW, Kim YM, Do EK, Park JH, Lee JS, Han J, Kim JH.** Macrophages regulate smooth muscle differentiation of mesenchymal stem cells via a prostaglandin F2alpha-mediated paracrine mechanism. *Arterioscler Thromb Vasc Biol* 32: 2733–2740, 2012.
36. **Li S, Wang DZ, Wang Z, Richardson JA, Olsen EN.** The serum response factor coactivator myocardin is required for vascular smooth muscle development. *Proc Natl Acad Sci USA* 100: 9366–9370, 2003.
37. **Liu C, Nath KA, Katusic ZS, Caplice NM.** Smooth muscle progenitor cells in vascular disease. *Trends Cardiovasc Med* 14: 288–293, 2004.
38. **Liu Y, Pleyte K, Knaus HG, Rusch NJ.** Increased expression of Ca^{2+}-sensitive K^+ channels in aorta of hypertensive rats. *Hypertension* 30: 1403–1409, 1997.
38a. **Long X, Tharp DL, Georger MA, Slivano OJ, Lee MY, Wamhoff BR, Bowles DK, Miano JM.** The smooth muscle cell-restricted KCNMB1 ion channel subunit is a direct transcriptional target of serum response factor and myocardin. *J Biol Chem* 284: 33671–33682, 2009.
39. **McGahon MK, Dash DP, Arora A, Wall N, Dawicki J, Simpson DA, Scholfield CN, McGeown JG, Curtis TM.** Diabetes downregulates large-conductance Ca^{2+}-activated potassium beta 1 channel subunit in retinal arteriolar smooth muscle. *Circ Res* 100: 703–711, 2007.
40. **McManus OB, Helms LM, Pallanck L, Ganetzky B, Swanson R, Leonard RJ.** Functional role of the beta subunit of high conductance calcium-activated potassium channels. *Neuron* 14: 645–650, 1995.
41. **Meredith AL, Thorneloe KS, Werner ME, Nelson MT, Aldrich RW.** Overactive bladder and incontinence in the absence of the BK large conductance Ca^{2+}-activated K^+ channel. *J Biol Chem* 279: 36746–36752, 2004.
42. **Moon HJ, Jeon ES, Kim YM, Lee MJ, Oh CK, Kim JH.** Sphingosylphosphorylcholine stimulates expression of fibronectin through TGF-beta1-Smad-dependent mechanism in human mesenchymal stem cells. *Int J Biochem Cell Biol* 39: 1224–1234, 2007.
43. **Moosmang S, Haider N, Bruderl B, Welling A, Hofmann F.** Antihypertensive effects of the putative T-type calcium channel antagonist mibefradil are mediated by the L-type calcium channel Cav1.2. *Circ Res* 98: 105–110, 2006.
44. **Moosmang S, Lenhardt P, Haider N, Hofmann F, Wegener JW.** Mouse models to study L-type calcium channel function. *Pharmacol Ther* 106: 347–355, 2005.
45. **Moosmang S, Schulla V, Welling A, Feil R, Feil S, Wegener JW, Hofmann F, Klugbauer N.** Dominant role of smooth muscle L-type calcium channel Cav1.2 for blood pressure regulation. *EMBO J* 22: 6027–6034, 2003.
46. **Narita Y, Yamawaki A, Kagami H, Ueda M, Ueda Y.** Effects of transforming growth factor-beta 1 and ascorbic acid on differentiation of human bone-marrow-derived mesenchymal stem cells into smooth muscle cell lineage. *Cell Tissue Res* 333: 449–459, 2008.
47. **Negishi Y, Kudo A, Obinata A, Kawashima K, Hirano H, Yanai N, Obinata M, Endo H.** Multipotency of a bone marrow stromal cell line, TBR31–2, established from ts-SV40 T antigen gene transgenic mice. *Biochem Biophys Res Commun* 268: 450–455, 2000.
48. **Nelson MT, Quayle JM.** Physiological roles and properties of potassium channels in arterial smooth muscle. *Am J Physiol Cell Physiol* 268: C799–C822, 1995.
49. **Owens GK, Kumar MS, Wamhoff BR.** Molecular regulation of vascular smooth muscle cell differentiation in development and disease. *Physiol Rev* 84: 767–801, 2004.
50. **Park KS, Jung KH, Kim SH, Kim KS, Choi MR, Kim Y, Chai YG.** Functional expression of ion channels in mesenchymal stem cells derived from umbilical cord vein. *Stem Cells* 25: 2044–2052, 2007.
51. **Park WS, Firth AL, Han J, Ko EA.** Patho-, physiological roles of voltage-dependent K^+ channels in pulmonary arterial smooth muscle cells. *J Smooth Muscle Res* 46: 89–105, 2010.
52. **Park WS, Son YK, Ko EA, Ko JH, Lee HA, Park KS, Earm YE.** The protein kinase C inhibitor, bisindolylmaleimide (I), inhibits voltage-dependent K^+ channels in coronary arterial smooth muscle cells. *Life Sci* 77: 512–527, 2005.
53. **Pittenger MF, Mackay AM, Beck SC, Jaiswal RK, Douglas R, Mosca JD, Moorman MA, Simonetti DW, Craig S, Marshak DR.** Multilineage potential of adult human mesenchymal stem cells. *Science* 284: 143–147, 1999.
54. **Prockop DJ.** Marrow stromal cells as stem cells for nonhematopoietic tissues. *Science* 276: 71–74, 1997.
55. **Sanchez-Ramos J, Song S, Cardozo-Pelaez F, Hazzi C, Stedeford T, Willing A, Freeman TB, Saporta S, Janssen W, Patel N, Cooper DR,**

Sanberg PR. Adult bone marrow stromal cells differentiate into neural cells in vitro. *Exp Neurol* 164: 247–256, 2000.
56. **Shanahan CM, Weissberg PL, Metcalfe JC.** Isolation of gene markers of differentiated and proliferating vascular smooth muscle cells. *Circ Res* 73: 193–204, 1993.
57. **Short B, Brouard N, Occhiodoro-Scott T, Ramakrishnan A, Simmons P.J.** Mesenchymal stem cells. *Arch Med Res* 34: 565–571, 2003.
58. **Toro L, Wallner M, Meera P, Tanaka Y.** Maxi-K(Ca), a unique member of the voltage-gated K channel superfamily. *News Physiol Sci* 13: 112–117, 1998.
59. **van Eys GJ, Voller MC, Timmer ED, Wehrens XH, Small JV, Schalken JA, Ramaekers FC, van der Loop FT.** Smoothelin expression characteristics: development of a smooth muscle cell in vitro system and identification of a vascular variant. *Cell Struct Funct* 22: 65–72, 1997.
60. **van Tuyn J, Knaan-Shanzer S, van de Watering MJ, de Graaf M, van der Laarse A, Schalij MJ, van der Wall EE, de Vries AA, Atsma DE.** Activation of cardiac and smooth muscle-specific genes in primary human cells after forced expression of human myocardin. *Cardiovasc Res* 67: 245–255, 2005.
61. **Ventura C.** Forced myocardin expression primes cardiac and smooth muscle transcription patterning in human mesenchymal stem cells. *Cardiovasc Res* 67: 182–183, 2005.
62. **Wamhoff BR, Bowles DK, Owens GK.** Excitation-transcription coupling in arterial smooth muscle. *Circ Res* 98: 868–878, 2006.
63. **Wang C, Yin S, Cen L, Liu Q, Liu W, Cao Y, Cui L.** Differentiation of adipose-derived stem cells into contractile smooth muscle cells induced by transforming growth factor-beta1 and bone morphogenetic protein-4. *Tissue Eng Part A* 16: 1201–1213, 2010.
64. **Wang D, Park JS, Chu JS, Krakowski A, Luo K, Chen DJ, Li S.** Proteomic profiling of bone marrow mesenchymal stem cells upon transforming growth factor beta1 stimulation. *J Biol Chem* 279: 43725–43734, 2004.
65. **Wang Z, Wang DZ, Pipes GC, Olson EN.** Myocardin is a master regulator of smooth muscle gene expression. *Proc Natl Acad Sci USA* 100: 7129–7134, 2003.
66. **Welling A, Ludwig A, Zimmer S, Klugbauer N, Flockerzi V, Hofmann F.** Alternatively spliced IS6 segments of the alpha 1C gene determine the tissue-specific dihydropyridine sensitivity of cardiac and vascular smooth muscle L-type Ca^{2+} channels. *Circ Res* 81: 526–532, 1997.
67. **Yuan XJ, Wang J, Juhaszova M, Golovina VA, Rubin LJ.** Molecular basis and function of voltage-gated K^+ channels in pulmonary arterial smooth muscle cells. *Am J Physiol Lung Cell Mol Physiol* 274: L621–L635, 1998.